Bioorganic & Medicinal Chemistry 19 (2011) 2508–2516

Contents lists available at ScienceDirect

Bioorganic & Medicinal Chemistry

journal homepage: www.elsevier.com/locate/bmc

Fluorescent phosphoinositide 3-kinase inhibitors suitable for monitoring of intracellular distribution

Donghee Kim [a], Hyunseung Lee [b], Hwiseok Jun [a], Soon-Sun Hong [b,*], Sungwoo Hong [a,*]

[a] Department of Chemistry, Korea Advanced Institute of Science and Technology (KAIST), Daejeon 305-701, Republic of Korea
[b] Department of Biomedical Sciences, College of Medicine, Inha University, Incheon 400-712, Republic of Korea

ARTICLE INFO

Article history:
Received 29 January 2011
Revised 9 March 2011
Accepted 10 March 2011
Available online 15 March 2011

Keywords:
Fluorescent PI3K inhibitor
Intracellular distribution
Anticancer
Drug design

ABSTRACT

The monitoring of the drug behavior and distribution in biological system can provide information whether drug reaches its desired target, and a biological rationale for the design of new therapeutics. We have developed a family of potent fluorescent PI3Kα inhibitors in which part of the fluorophore was engineered to be a pharmacophore capable of inhibiting PI3Kα. These xanthine derivatives are characterized by a donor–acceptor molecular structure, and changes in the electronic properties of the two variation points at R_1 and R_2 give rise to notable bathochromic shifts in the $\lambda_{em,\,abs}$ and increase the value of Φ_F. Further, we illustrated the use of **E2** (PI3Kα/IC_{50} = 0.068 μM, T47D cell viability: IC_{50} = 0.9 μM) to block cancer cell proliferation and to monitor its subcellular localization by fluorescence microscopy.

1. Introduction

An understanding of intracellular drug distribution and its fate in biological systems is of enormous value for several reasons. Primarily, it is important to confirm that drug molecules reach their desired target inside cells. The knowledge of drug concentration and metabolism as a function of time is also important for optimizing treatment time, determining the selectivity of the drug for various sites and customizing medicine for therapy. In addition, information regarding the receptors and particular subcellular compartments with which drugs are associated is useful, because it may reveal mechanisms of action/deactivation/resistance[1] and provide a biological rationale for the design of new therapeutics with improved properties and fewer side effects.[2]

Monitoring the drug distribution, concentration and pathways travelled by drug molecules has proven still challenging, and is often accomplished only indirectly from serum pharmacokinetic studies. The tethering of fluorescent dyes to drugs (Fig. 1, up) is a popular method for visual monitoring the time course of the drug behavior,[3] and also provides a useful tool for studying cellular, animal and clinical imaging in a noninvasive and nonradioactive procedure.[4] Thus, light is used to excite the fluorophore part of tag conjugated drug, and its emission from within the cells can be readily observed by confocal microscopy. The addition of fluorophores into the drug molecules, however, often causes undesired effects on binding affinity, cell permeability, in vivo activity and toxicity. The ability of fluorophore-conjugated compounds to adequately imitate the drug molecules is also questionable, and their movement/distribution/metabolism might be different to those of parent drug. In addition, there is concern that the fluorophore tag might be detached from the drug molecules in the intracellular environment, resulting in the cleaved fluorophore alone being probed.[5] In this sense, an emissive drug (Fig. 1, down) can be considered as an ideal species for tracking its translocation and disposition in cells or even in tissues, and this optical method could be potentially applied to the study of drug pharmacokinetics and the mechanism of action.

Phosphoinositide 3-kinases (PI3Ks) are lipid kinases that catalyze phosphorylation of the 3-hydroxyl position of PIP2 (phosphatidylinositol 4,5-diphosphate) to PIP3 (phosphatidylinositol 3,4,5-triphosphate). The resulting second messenger, PIP3 can regulate multiple physiological processes, including cell growth, differentiation, survival, and motility.[6] PI3Kα has emerged as an attractive target for cancer treatment because the amplification of PI3Kα is one of the most common molecular findings in human malignancies,[7] and several PI3Kα inhibitors are currently under evaluation in human clinical trials.[8] As substantial structural and biochemical information about PI3 kinases is available, PI3Kα represents one of good targets for structure-based drug design to facilitate the discovery of potent inhibitors. We envisioned that cell-permeable fluorescent PI3Kα inhibitors could allow their subcellular localization to be monitored in live cells by fluorescence microscopy. Herein, we report fluorescent PI3K inhibitors in which some part of the fluorophore was engineered to be a

* Corresponding authors. Tel.: +82 32 890 3683; fax: +82 32 890 2462 (S.-S.H.); tel.: +82 42 350 2811; fax: +82 42 350 2810 (S.H.).
E-mail addresses: hongorg@kaist.ac.kr (S.-S. Hong), hongs@inha.ac.kr (S. Hong).

0968-0896/$ - see front matter © 2011 Elsevier Ltd. All rights reserved.
doi:10.1016/j.bmc.2011.03.025

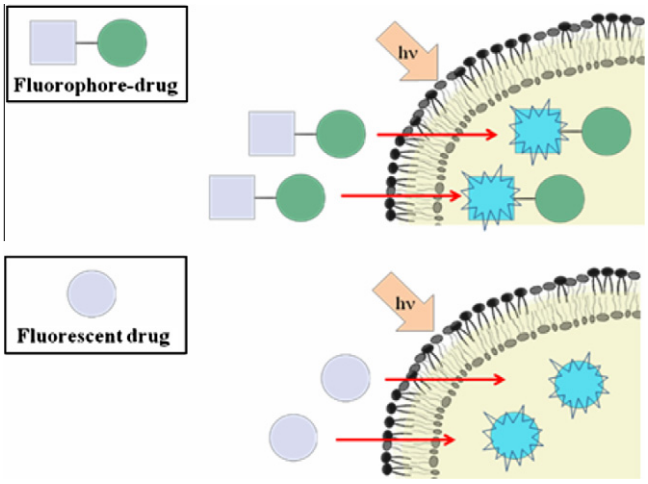

Figure 1. Design of an azaindole scaffold as PI3K inhibitor and opportunities for modification.

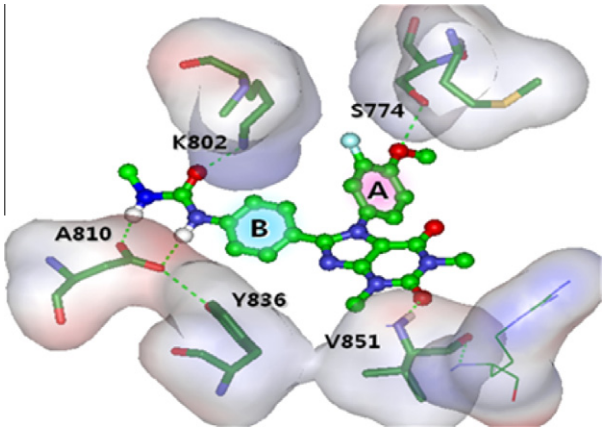

Figure 2. Putative binding mode of **D3** docked into p110α the catalytic subunit of PI3Kα homology model. The carbonyl oxygen seems to form an interaction with the hinge (Val851). Selected residues (S774, K802, A810, and Y836) are shown for possible interaction with A or B aromatic subunits.

pharmacophore capable of inhibiting PI3 kinases, and describe the bioapplication of our compound in the monitoring intracellular distribution by microscopic study.

2. Results and discussion

2.1. Chemistry

Our prior work showed fluorescent kinase inhibitors can be prepared from a xanthine scaffold,[9] but these earlier compounds did not possess appropriate properties to be useful for cellular imaging. To identify the optimized compounds that could be used for these applications, we initiated a program to enhance both biological and photophysical profiles of fluorescent PI3Kα inhibitors. The synthetic strategy was based on a versatile combination of regioselective N7-arylation and direct C8-arylation as shown in Scheme 1. Both A and B aromatic subunits are easily functionalized with either electron-acceptor or electron-donor groups, facilitating our rational approach to building fluorescent PI3Kα inhibitors for improving photophysical, physicochemical properties and biological activity. A variety of analogues exhibiting fluorescence were synthesized and screened for both PI3K inhibition in vitro and in cancer cells.

2.2. PI3K enzyme activity

Analysis of the structure docked into the p110α homology model[10] suggests that the xanthine skeleton maintains the hydrogen-bonding pattern with V851 and is lined by Y836 and A810. Based on considerations regarding space and environmental polarity of ATP binding in PI3Kα compounds incorporating groups at the A and B were designed to estimate experimentally the energetic gains in binding free enthalpy resulting from filling the space of the hydrophobic pocket. We first explored the optimal group which best fits the space of N7 region, focusing on structural modification of A subunit. N7-Aryl ring is critical for activity, and corresponding analogues containing either N7-benzyl or alkyl groups show no activity over PI3K. Clearly, the significant increase in potency of **A3** (IC_{50} = 0.15 μM)[11] compared to that of **C1** (IC_{50} = 12.5 μM) may be related to the hydrogen bonding interaction of the *p*-OMe group with S774 (Fig. 2). Guided by SAR trends and molecular modeling, an array of various substitutents on A aryl ring was progressed. The presence of 3,4-diCl groups on this ring resulted in compounds which were generally of equivalent enzyme potency or better enzyme potency than the corresponding *p*-OMe derivatives (Table 1). Profound effects on potency were achieved with compounds incorporating *m*-F, *p*-OMe phenyl group at N7, and **D2** was the earliest example in the xanthine series to display potency over PI3Kα enzyme at double-digit nanomolar concentration (IC_{50} = 31 nM). Building upon the success observed with on aryl group, an investigation of the effect of the appendage at C8 position was conducted. We focused in our design towards the introduction of a hydrogen bond accepting group (e.g., amide, carbamate or urea) on the B ring to further probe the interaction with K802, A810 and Y836. Among the numerous synthesized compounds, **A4, D2, D3, E2**, and **G2** exhibited excellent potencies over PI3Kα as shown in Table 1. Notably, the highest PI3Kα potency was obtained with urea group (**D3**: IC_{50} = 17 nM). Molecular modeling of **D3**, as shown in Figure 2, displays the crucial hydrogen bonding interactions, including the xanthine carbonyl group binding to the hinge region V851 and the methoxy group binding to S774. In addition, the urea moiety of **D3** forms two hydrogen-bonding interactions to A810 through both urea–NH groups and one to the catalytic lysine (K802) through the urea carbonyl group. Some sulfonamide moieties (e.g., **A7** and **A8)** are also well tolerated, and good activity was observed (Table 1).

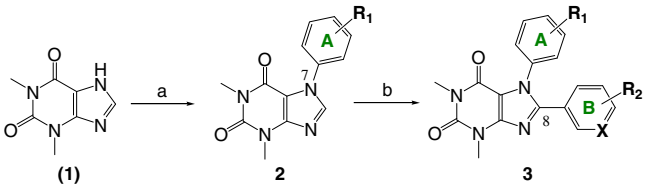

Scheme 1. Reagents and conditions: (a) $Cu(OAc)_2$, pyridine, arylboronic acid, CH_2Cl_2, 40 °C; (b) $Pd(OAc)_2$, CuI, Cs_2CO_3, aryl bromide, DMF, 130 °C.

2.3. Cellular activity

Given the impressive enzyme activity profile, several compounds from this series were further tested for cellular proliferation activity against cancer cell lines. To measure the inhibitory effect of compounds on cell growth, cell viability was tested by 3-(4,5-dimethylthiazol-2-yl)-2,5-diphenyltetrazolium bromide (MTT) assay in T47D, SK-BR3, and MCF-7 human breast cancer cell cultures. Several of inhibitors showed antiproliferative effects and **A4**, **D2** and **E2** showed potent antiproliferative effects at micromolar concentration (Table 2).

Table 1
PI3Kα inhibitory activity of representative xanthine analogues[a]

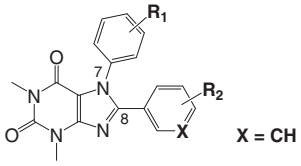

Compd	R_1	R_2	λ_{max}[a] (nm)	λ_{em}[b] (nm)	Φ_F[c]	IC_{50}[d] (μM)
A1	*p*-OMe	*p*-NMe_2	348	428	0.034	22
A2	*p*-OMe	*m*-$NHSO_2Me$	310	419	0.003	3.2
A3	*p*-OMe	*p*-NHAc	319	409	0.013	0.15
A4	*p*-OMe	*p*-$NHCO_2Me$	320	391	0.15	0.21
A5[e]	*p*-OMe	4-$NHSO_2Me$	320	405	0.037	>30
A6[e]	*p*-OMe	5-$NHSO_2Me$	322	410	0.013	4.5
A7[e]	*p*-OMe	5-$NHSO_2Ph$	323	410	0.029	0.091
A8[e]	*p*-OMe	5-$NHSO_2Tol$	322	413	0.035	0.22
B1	3,4-diOMe	*p*-NMe_2	315	414	0.22	25
B2	3,4-diOMe	*p*-NHAc	319	401	0.034	0.51
C1	H	*p*-NHAc	320	390	0.076	12.5
C2	*p*-Me	*p*-NHAc	315	381	0.015	0.37
D1	*m*-F, *p*-OMe	*p*-NMe_2	348	433	0.37	22
D2	*m*-F, *p*-OMe	*p*-NHAc	320	411	0.016	0.031
D3	*m*-F, *p*-OMe	*p*-NHCONHMe	310	413	0.028	0.017
D4	*m*-F, *p*-OMe	*m*-OMe, *p*-NHAc	328	409	0.049	8.5
E1	*m*-F	*p*-NMe_2	350	445	0.63	20
E2	*m*-F	*p*-NHAc	338	430	0.12	0.068
E3	*m*-F	*o*-OMe, *p*-NMe_2	337	428	0.79	22
F1	3,5-DiF	*p*-NMe_2	348	439	0.92	25
F2	3,5-DiF	*o*-OMe, *p*-NMe_2	327	433	0.65	15
G1	3,4-DiCl	*p*-NMe_2	347	444	0.59	>30
G2	3,4-DiCl	*p*-NHAc	320	401	0.094	0.28
G3	3,4-DiCl	*o*-OMe, *p*-NHAc	293	406	0.023	13

[a] Only the longest absorption maxima are shown.
[b] Excited at the maximum excitation wavelength.
[c] Absolute fluorescence quantum yield.
[d] IC_{50} values over PI3Kα determined using PI3-Kinase Glo kit (Promega-inc). Data are mean values for two independent experiments performed in duplicate with standard error of <20%.
[e] X = N.

Table 2
Cancer cell proliferation of selected xanthine derivatives

Compd	Growth IC_{50} (μM)		
	T47D	MCF7	SK-BR3
A3	3.7	9.4	>25
A4	1.7	4.2	>25
D2	1.6	2.8	11.5
D3	4.7	11.6	>25
E2	0.9	1.7	15.4

2.4. Fluorescence property

Having successfully identified the potent PI3K inhibitors, we next turned to the investigation of their photonic properties. The fluorescent xanthine structure seems to undergo intramolecular charge transfer from the C8-aryl ring to the electron-deficient xanthine core upon excitation by light.[12] For a rational design through theoretical calculation, the orbital shapes of the highest occupied molecular orbital (HOMO) and the lowest unoccupied molecular orbital (LUMO) of xanthine core skeleton were examined, focusing on the substitution patterns. Since the *p*-R_2 position at the LUMO has a smaller lobe than that at the HOMO, we reasoned that the introduction of an electron-donating group on the *p*-R_2 position could trigger a bathochromic shift in our compounds (Fig. 3). In addition, electronic perturbation of the substituents at the R_1 position on the fluorescence properties was observed. LUMO of N7 aryl group with an electron withdrawing substituent R_1 has significant larger lobes, and the delocalization of the π orbital seems to be facilitated by an electron withdrawing group on R_1. The bathochromic shift of emission wavelengths is well consistent with our prediction based on the quantum mechanics calculation (Table 2). For instance, a direct comparison of **C2** (R_1 = *p*-Me, R_2 = *p*-NHAc:

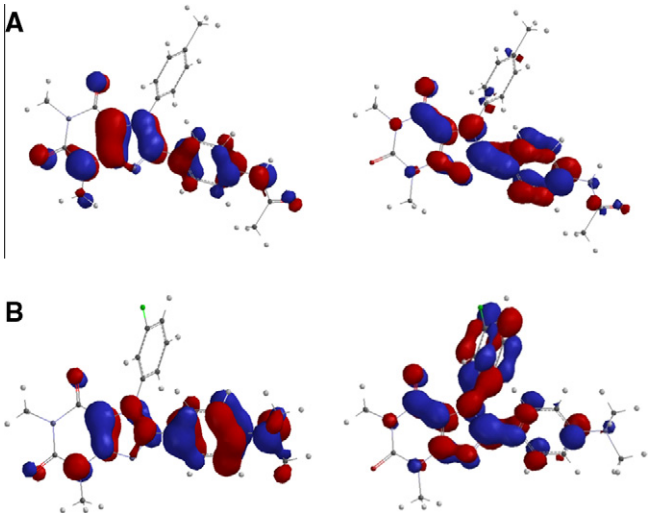

Figure 3. HOMO–LUMO electron distribution diagrams. (Calculated and evaluated from Spartan '04 software, Wavefunction Inc.) (A) HOMO (left) and LUMO (right) of **C2**. (B) HOMO (left) and LUMO (right) of **E1**. Tubular network formation of HUVECs by treatment with DMSO (control) and **B3** (0.1, 1 and 10 μM).

λ_{em} = 381 nm, Φ_F = 0.015) with **E1** (R_1 = *m*-F, R_2 = *p*-NMe_2: λ_{em} = 445 nm, Φ_F = 0.63) clearly reveals that changes in the electronic properties of the two variation points at R_1 and R_2 give rise to notable bathochromic shifts in the $\lambda_{em,\ abs}$ and increase the value of Φ_F.[13]

To trigger a bathochromic shift of inhibitors, efforts focused on a search for *p*-OMe surrogates that could withdraw electrons of N7-aryl ring while maintaining the hydrogen bonding interaction. The presence of *m*-F resulted in compounds which were generally of equivalent or better enzyme potency than the corresponding *p*-OMe derivatives. **E2** was the first example in the xanthine series to display potency over PI3Kα enzyme at double-digit nanomolar concentration (IC_{50} = 68 nM) with a moderate quantum yield (Φ_F = 0.12).

2.5. Intracellular monitoring studies by confocal microscopy

Among our new fluorescent inhibitors, we chose **E2** as an imaging agent for cancer cells, because it shows good PI3Kα (IC_{50} = 0.068 μM), cell-based antiproliferative activity (IC_{50} = 0.9 μM) and reasonable photophysical properties. When T47D breast cancer cells were incubated with **E2** for 1 h, fluorescence became clearly visible in the cytoplasm of T47D cells, providing visual evidence of the compound entering cells and information on the intracellular distribution pattern (Fig. 4).

Furthermore, at 48 h after treatment, fluorescence images of the cells revealed severe morphological changes such as shrinkage, elongation, or a disorder in cell shape (Fig. 5), suggesting that this approach can also be useful for monitoring the antiproliferative

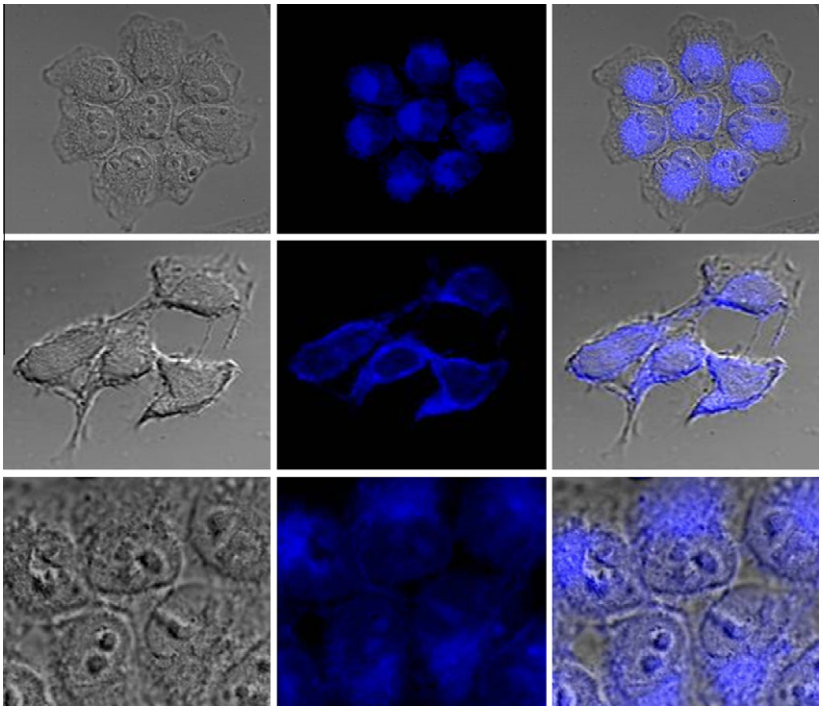

Figure 4. Confocal microscopic observation of the intracellular **E2** disposition in T47D breast cancer cells. T47D cells were incubated with 5 μM solution of **E2** for 1 h. Left: transmitted light image; middle: fluorescence microscopic image; right: overlaid image.

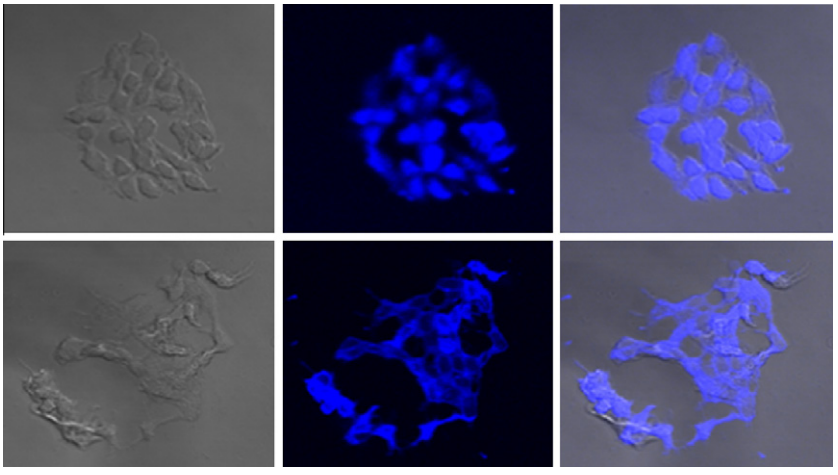

Figure 5. Confocal microscopic observation of the intracellular **E2** (5 μM) disposition in T47D breast cancer cells. Up: cells at 24 h after treatment; down: cells at 48 h after treatment.

processes in cancer cells associated with drug retention and concentration as a function of time.

3. Conclusion

In summary, we prepared a family of xanthine derivatives serving as a dual function in exhibiting fluorescence and inhibiting PI3Ks. Further, we have successfully demonstrated the use of **E2** to block cancer cell proliferation and to monitor its subcellular localization by fluorescence microscopy. These combined features of PI3K inhibitors would be useful in biological or pharmaceutical research to get early feedback on treatment efficacy or, potentially, for imaging in a clinical setting to anticipate the therapeutic process.

4. Experimental section

4.1. Chemical preparation

4.1.1. General chemistry

Unless stated otherwise, reactions were performed in flame-dried glassware under a positive pressure of nitrogen using freshly distilled solvents. Analytical thin layer chromatography (TLC) was performed on precoated Silica Gel 60 F_{254} plates and visualization on TLC was achieved by UV light (254 and 354 nm). Flash column chromatography was undertaken on Silica Gel (400–630 mesh). ^{1}H NMR was recorded on 400 MHz or 300 MHz and chemical shifts were quoted in parts per million (ppm) referenced to the appropriate solvent peak or 0.0 ppm for tetramethylsilane. The following abbreviations were used to describe peak splitting patterns when appropriate: br = broad, s = singlet, d = doublet, t = triplet, q = quartet, m = multiplet, dd = doublet of doublet. Coupling constants, *J*, were reported in hertz unit (Hz). Chemical shifts were reported in ppm referenced to the center line of a triplet at 77.0 ppm of chloroform-*d*. Mass spectral data were obtained from the KAIST Basic Science Institute by using EI method. If needed, products were purified via a Waters semi-preparative HPLC equipped with an Agilent Prep-C18 reverse phase column (21.2 × 150 mm, 10 mm). The mobile phase was a mixture of MeOH (0.1% TFA) and H_2O (0.1% TFA). Commercial grade reagents and solvents were used without further purification except as indicated below. Dichloromethane was distilled from calcium hydride. THF was distilled from sodium. Unless otherwise stated, all commercial reagents and solvents were used without additional purification.

4.1.2. General procedure 1. (GP1)

To a solution of theophylline (2 equiv), 4-methoxyphenyl boronic acid (1 equiv), copper(II) acetate (2.2 equiv) in dichloromethane was added pyridine (5 equiv) and the entire solution was left stirring at 40 °C for 24 h. The solution was then filtered through a pad of Celite, and the filterate was concentrated under reduced pressure. The filtrate was washed with dichloromethane, H_2O, and dried ($MgSO_4$). The solvent was concentrated in vacuo and desired products were purified either by recrystallization or flash column chromatography.

4.1.3. 7-(4-Methoxyphenyl)-1,3-dimethyl-1H-purine-2,6(3H,7H)-dione

Starting from theophylline (1.0 g, 5.55 mmol), 4-methoxyphenyl boronic acid (420 mg, 2.77 mmol), copper(II) acetate (1.1 g, 6.11 mmol) in dichloromethane (10 mL), pyridine (1.12 mL, 13.88 mmol) and following the GP1, the desired aryl xanthine was isolated (477 mg, 60%); ^{1}H NMR δ (300 MHz, $CDCl_3$): 3.38 (3H, s), 3.64 (3H, s), 3.85 (3H, s), 6.98 (2H, d, J = 6 Hz), 7.36 (2H, d, J = 6 Hz), 7.68 (1H, s); ^{13}C NMR δ (75 MHz, $CDCl_3$): 28.18, 29.95, 55.68, 107.50, 114.43, 126.51, 127.78, 141.28, 149.41, 151.65, 154.52, 160.11; LR-MS (EI+) m/z calcd for $C_{14}H_{15}N_4O_3$ $[M+H]^+$: 287.1, found: 287.1.

4.1.4. 7-(3,4-Dimethoxyphenyl)-1,3-dimethyl-1H-purine-2,6(3H,7H)-dione

Starting from 3,5-dimethoxyphenyl boronic acid (1.5 g, 8.33 mmol), theophylline (1.0 g, 5.55 mmol), copper(II) acetate (1.5 g, 8.33 mmol) and pyridine (1.1 mL, 13.9 mmol) in DCM and following the GP1, the desired aryl xanthine was isolated the desired aryl xanthine (787 mg, 45%); ^{1}H NMR δ (300 MHz, $CDCl_3$): 3.38 (3H, s), 3.64 (3H, s), 3.90 (3H, s), 3.92 (3H, s), 6.92 (1H, d), 6.97 (1H, d), 7.00 (1H, d); ^{13}C NMR δ (75 MHz, $CDCl_3$): 28.28, 29.99, 56.29, 56.36, 107.61, 109.47, 111.03, 117.38, 128.01, 141.36, 149.36, 149.50, 149.86, 151.71, 154.52; HRMS (ESI+) m/z calcd for $C_{15}H_{15}NaN_4O_4$ $[M+Na]^+$: 339.1069, found: 339.1049.

4.1.5. 1,3-Dimethyl-7-phenyl-1H-purine-2,6(3H,7H)-dione

Starting from phenyl boronic acid (1.0 g, 8.33 mmol), theophylline (1.0 g, 5.55 mmol), copper(II) acetate (1.5 g, 8.33 mmol) and pyridine (1.1 mL, 13.9 mmol) in DCM and following the GP1, the desired aryl xanthine was isolated the desired aryl xanthine (633 mg, 45%); ^{1}H NMR δ (300 MHz, $CDCl_3$): 3.36 (3H, s), 3.62 (3H, s), 7.46 (5H, m) 7.72 (1H, s); ^{13}C NMR δ (75 MHz, $CDCl_3$): 28.20, 29.95, 107.21, 125.10, 129.12, 129.28, 134.85, 141.26, 149.67, 151.57, 154.41; HRMS (ESI+) m/z calcd for $C_{13}H_{11}NaN_4O_2$ $[M+Na]^+$: 279.0858, found: 279.0850.

4.1.6. 1,3-Dimethyl-7-p-tolyl-1H-purine-2,6(3H,7H)-dione

Starting from theophylline (1.0 g, 5.55 mmol), 4-methylphenyl boronic acid (906 mg, 6.66 mmol), copper(II) acetate (1.8 g, 9.99 mmol) in dichloromethane (30 mL) and pyridine (1.34 mL, 16.65 mmol) and following the GP1, the desired aryl xanthine was isolated the desired aryl xanthine (98 mg, 65%); ^{1}H NMR δ (300 MHz, DMSO-d_6): 2.39 (3H, s), 3.21 (3H, s), 3.48 (3H, s), 7.32 (2H, d, J = 8.3 Hz), 7.43 (2H, d, J = 8.3 Hz), 8.32 (1H, s); ^{13}C NMR δ (75 MHz, $CDCl_3$): 21.31, 28.29, 30.04, 107.48, 125.07, 129.96, 132.46, 139.50, 141.26, 149.64, 151.75, 154.57; HRMS (EI+) m/z calcd for $C_{14}H_{15}N_4O_2$ $[M+H]^+$: 271.1195, found: 271.1152.

4.1.7. 7-(3-Fluoro-4-methoxyphenyl)-1,3-dimethyl-1H-purine-2,6(3H,7H)-dione

Starting from 3-fluoro-4-methoxy-phenylboronic acid (1.078 g, 6.66 mmol), theophylline (1.0 g, 5.55 mmol), copper(II) acetate (1.15 g, 6.66 mmol) in DCM and following the GP1, the desired aryl xanthine was isolated the desired aryl xanthine (1.03 g, 61%); ^{1}H NMR δ (400 MHz, $CDCl_3$): 3.36 (3H, s), 3.61 (3H, s), 3.91 (3H, s), 7.02 (1H, t), 7.20 (2H, t), 7.66 (1H, s); ^{13}C NMR δ (100 MHz, $CDCl_3$): 28.28, 30.03, 56.62, 107.45, 113.90, 121.36, 127.51, 141.27, 148.57, 149.58, 150.64, 151.64, 153.12, 154.51; HRMS (ESI+) m/z calcd for $C_{14}H_{14}FN_4O_3$ $[M+H]^+$: 305.1050, found: 305.1031.

4.1.8. 7-(3-Fluorophenyl)-1,3-dimethyl-1H-purine-2,6(3H,7H)-dione

Starting from theophyline (500 mg, 2.77 mmol), 3-fluorophenylboronic acid (466 mg, 3.33 mmol), copper(II) acetate (603 mg, 3.33 mmol) in dichloromethane (40 mL), pyridine (0.56 mL, 6.94 mmol) and following the GP1, the desired aryl xanthine was isolated the desired aryl xanthine (303 mg, 44%); ^{1}H NMR δ (300 MHz, $CDCl_3$); 3.51 (3H, s), 3.62 (3H, s), 7.14 (1H, t), 7.20 (1H, t), 7.24 (1H, t), 7.44 (1H, q), 7.82 (1H, s); ^{13}C NMR δ (75 MHz, $CDCl_3$): 28.17, 29.90, 106.99, 112.67, 115.99, 120.66, 135.82, 141.07, 149.70, 151.41, 154.26, 160.82, 164.11; HRMS (EI+) m/z calcd for $C_{13}H_{12}FN_4O_2$ $[M+H]^+$: 275.0944, found: 275.0945.

4.1.9. 7-(3,5-Difluorophenyl)-1,3-dimethyl-1H-purine-2,6(3H,7H)-dione

Starting from 3,5-difluorophenyl boronic acid (1.3 g, 8.33 mmol) was reacted with theophylline (1.0 g, 5.55 mmol), copper(II) acetate (1.5 g, 8.33 mmol) and pyridine (1.1 mL, 13.9 mmol) in DCM and following the GP1, the desired aryl xanthine was isolated the desired aryl xanthine (1.2 g, 75%); ^{1}H NMR δ (300 MHz, DMSO-d_6): 3.23 (3H, s), 3.49 (3H, s), 7.43 (1H, m), 7.49 (2H, d), 8.45 (1H, s); ^{13}C NMR δ (100 MHz, DMSO-d_6): 27.14, 28.86, 103.18, 105.76, 108.50, 136.35, 142.20, 149.17, 150.40, 153.21, 161.49 (dd); HRMS (ESI+) m/z calcd for $C_{13}H_9F_2NaN_4O_2$ $[M+Na]^+$: 315.0670, found: 315.0660.

4.1.10. General procedure 2 (GP2)

To a solution xanthine (1 equiv), aryl bromide (1.5 equiv), copper (I) iodide (3 equiv) and palladium(II) acetate (20 mol %) in anhydrous DMF was added cesium carbonate (2.5 equiv) and the solution was set in a sealed tube. Reactions were carried out at about 130 °C for 40 h under nitrogen purged status. The solution was filtered through Celite to remove palladium. The filtrate was washed with dichloromethane, H_2O, and dried ($MgSO_4$). The solvent was concentrated in vacuo and desired products were purified either by flash column chromatography or reverse phase HPLC.

4.1.11. 8-(4-(Dimethylamino)phenyl)-7-(4-methoxyphenyl)-1,3-dimethyl-1H-purine-2,6-(3H,7H)-dione (A1)

Aryl xanthine (40 mg, 0.14 mmol) was reacted with 4-bromo-*N,N*-dimethylaniline (42 mg, 0.21 mmol) according to GP2 to give the desired dimethylanline **A1** (44 mg, 78%) by recrystallization from CH_2Cl_2 and hexane; ^{1}H NMR δ (300 MHz, $CDCl_3$): 3.01 (6H, s), 3.33 (3H, s), 3.67 (3H, s), 3.75 (3H, s), 3.83 (3H, s), 6.50 (2H, d), 6.92 (2H, d), 7.23 (2H, d), 7.32 (2H, d); ^{13}C NMR δ (75 MHz, $CDCl_3$): 28.04, 29.96, 40.14, 55.62, 108.95, 111.46, 114.56, 115.56, 128.99, 129.39, 130.38, 148.96, 151.24, 151.97, 152.48, 154.54, 160.01; HRMS (EI+) m/z calcd for $C_{22}H_{24}N_5O_3$ $[M+H]^+$: 406.1879, found: 406.1879.

4.1.12. N-(3-(7-(4-Methoxyphenyl)-1,3-dimethyl-2,6-dioxo-2,3,-6,7-tetrahydro-1H-purin-8-yl)phenyl)-methanesulfonamide (A2)

7-(4-Methoxyphenyl)-1,3-dimethyl-1*H*-purine-2,6(3H,7H)-dione (100 mg, 0.349 mmol) was reacted with *N*-(3-bromophenyl)-*N*-(methylsulfonyl)methanesulfonamide(172 mg, 0.524 to GP2. (92 mg, 58%). After removal of palladium by filteration through Celite, solution was washed and dried. The residue was purified by flash column chromatography (CH_2Cl_2/MeOH, 20:1) to produce the desired sulfonamide **A2** (27 mg, 51%); ^{1}H NMR δ (300 MHz, DMSO-d_6): 2.83 (3H, s), 3.18 (3H, s), 3.53 (3H, s), 3.80 (3H, s), 6.98 (2H, d), 7.05 (1H, d), 7.18 (1H, d), 7.29 (1H, s), 7.30 (2H, d), 7.39 (1H, s), 9.92 (1H, s); ^{13}C NMR δ (75 MHz, DMSO-d_6): 28.08, 29.98, 55.33, 55.90, 109.48, 114.65, 120.29, 121.53, 124.46, 128.61, 129.44, 132.50, 139.25, 148.25, 150.49, 151.40, 154.01, 159.98, 167.00; HR-MS (ESI+) m/z calcd for $C_{21}H_{22}N_5O5_S$ $[M+H]^+$: 456.1336, found: 456.1355.

4.1.13. N-(4-(7-(4-Methoxyphenyl)-1,3-dimethyl-2,6-dioxo-2,3,6,7-tetrahydro-1H-purin-8-yl)phenyl)-acetamide (A3)

Aryl xanthine (101 mg, 0.34 mmol) was reacted with *N*-(4-bromophenyl)acetamide (112 mg, 0.52 mmol) according to GP2. After removal of palladium by filteration through Celite, solution was washed and dried. Crude product was recrystallized from chloroform and diethyl ether to and the residue was subjected to HPLC separation to give the desired amide **A3** (128 mg, 90%); ^{1}H NMR δ (300 MHz, $CDCl_3$): 2.16 (3H, s), 3.37 (3H, s), 3.70 (3H, s), 3.85 (3H, s), 6.93 (2H, d, J = 9 Hz), 7.21 (2H, d, J = 9 Hz), 7.45 (4H, m); ^{13}C NMR δ (75 MHz, $CDCl_3$): 14.25, 22.83, 24.85, 28.16, 29.84, 30.02, 55.65, 109.49, 114.69, 119.22, 128.61, 128.83, 130.20, 139.61, 148.74, 151.88, 154.67, 160.29; HRMS (EI+) m/z calcd for $C_{22}H_{22}N_5O_4$ $[M+H]^+$: 420.1672, found: 420.1668.

4.1.14. Methyl-4-(7-(4-methoxyphenyl)-1,3-dimethyl-2,6-dioxo-2,3,6,7-tetrahydro-1H-purin-8-yl)phenyl carbamate (A4)

Aryl xanthine (35 mg, 0.125 mmol) was reacted with methyl 4-bromophenylcarbamate (42 mg, 0.184 mmol) according to GP2. The residue was purified by flash column chromatography (EtOAc/CH_2Cl_2, 1:20) to produce the desired carbarmate **A4** (27 mg, 51%); ^{1}H NMR δ (300 MHz, $CDCl_3$): 2.26 (3H, s), 2.40 (3H, s), 3.34 (3H, s), 3.67 (3H, s), 7.15 (2H, d, J = 9 Hz), 7.21 (2H, d, J = 9 Hz), 7.41 (4H, s); ^{13}C NMR δ (75 MHz, $CDCl_3$): 21.26, 24.00, 27.64, 29.63, 109.00, 118.95, 124.00, 127.24, 129.94, 131.00, 133.13, 139.41, 139.65, 148.57, 150.50, 150.60, 151.65, 168.00; LRMS (EI+) m/z calcd for $C_{21}H_{18}N_5O_4$ $[M-OMe]^+$: 404.1, found: 404.1.

4.1.15. N-(5-(7-(4-Methoxyphenyl)-1,3-dimethyl-2,6-dioxo-2,3,6,7-tetrahydro-1H-purin-8-yl)pyridin-2-yl)methanesulfonamide (A5)

7-(4-Methoxyphenyl)-1,3-dimethyl-1*H*-purine-2,6(3H,7H)-dione(80 mg, 0.279 mmol) was reacted with *N*-(5-bromopyridin-2-yl)-*N*-(methylsulfonyl)methanesulfonamide(138 mg, 0.986 mmol) according to GP2. After removal of palladium by filteration through Celite, solution was washed and dried. Crude product was recrystalized by MC and the residue was subjected to HPLC separation to give desired sulfonamide **A5** (82 mg, 64%); ^{1}H NMR δ (300 MHz, CHCl-**D1**): 3.09(2H, s), 3.34(2H, s), 3.66(3H, s), 3.84(3H, s), 6.96(2H, d), 7.22(2H, d), 7.78(1H, d), 8.42(1H, bs), 10.43(1H, bs); ^{13}C NMR δ (75 MHz, CHCl-**D1**): 27.93, 29.79, 41.06, 55.44, 109.68, 111.80, 114.85, 127.56, 128.43, 139.73, 146.35, 147.40, 148.40, 151.48, 149.40. 145.30, 160.37; HR-MS (ESI+) m/z calcd for $C_{20}H_{21}N_6O_5S$ $[M+H]^+$: 457.1294, found: 457.1340.

4.1.16. N-(5-(7-(4-Methoxyphenyl)-1,3-dimethyl-2,6-dioxo-2,3,6,7-tetrahydro-1H-purin-8-yl)pyridin-3-yl)methanesulfonamide (A6)

Aryl xanthine (70 mg, 0.25 mmol) was reacted with *N*-(5-bromopyridin-3-yl)-*N*-(methylsulfonyl)methanesulfonamide (92 mg, 0.37 mmol) according to GP2. The residue was purified by flash column chromatography (CH_2Cl_2/MeOH, 10:1) to produce the desired sulfonamide **A6** (55 mg, 48%); ^{1}H NMR δ (300 MHz, $CDCl_3$): 2.90 (3H, s), 3.35 (3H, s), 3.67 (3H, s), 3.82 (3H, s), 6.95 (2H, d), 7.22 (2H, d), 8,36 (1H, s), 8,71 (1H, s); ^{13}C NMR δ (75 MHz, $CDCl_3$): 28.11, 29.96, 40.22, 55.60, 110.16, 114.97, 126.71, 127.59, 128.57, 142.17, 145.92, 147.25, 148.48, 151.57, 154.46, 160.58; HRMS (EI+) m/z calcd for $C_{20}H_{21}N_6O_5S$ $[M+H]^+$: 457.1294, found: 457.1299.

4.1.17. N-(5-(7-(4-Methoxyphenyl)-1,3-dimethyl-2,6-dioxo-2,3,6,7-tetrahydro-1H-purin-8-yl)pyridin-3-yl)benzenesulfonamide (A7)

Aryl xanthine (100 mg, 0.367 mmol) was reacted with *N*-(5-bromopyridin-3-yl)-*N*-(phenylsulfonyl)benzenesulfonamide (250 mg, 0.551 mmol) according to GP2. The residue was purified by flash column chromatography (EtOAc/CH_2Cl_2, 4:1) to produce the desired sulfonamide **A7** (114 mg, 60%); ^{1}H NMR δ (300 MHz, $CDCl_3$): 3.35 (3H, s), 3.66 (3H, s), 3.81 (3H, s), 6.93 (2H, d, J = 9 Hz), 7.17 (2H, d, J = 6 Hz), 7.54 (1H, t, J = 9 Hz), 7.66 (2H, d, J = 9 Hz), 7.72 (1H, t, J = 3 Hz), 8.81 (1H, d, J = 2.4 Hz), 8.42 (1H, d, J = 3 Hz); ^{13}C NMR δ (75 MHz, $CDCl_3$): 28.06, 29.86, 55.49, 110.08, 114.89, 125.38, 126.98, 127.40, 128.07, 128.07, 128.39, 129.25, 133.27, 133.48, 138.63, 142.69, 145.80, 147.36, 148.40, 151.53, 154.40, 160.52; HRMS (EI+) m/z calcd for $C_{25}H_{23}N_6O_5S$ $[M+H]^+$: 519.1450, found: 519.1460.

N-(5-(7-(4-methoxyphenyl)-1,3-dimethyl-2,6-dioxo-2,3,6,7-tetrahydro-1H-purin-8-yl)pyridin-3-yl)-4-methylbenzenesulfonamide (**A8**). Aryl xanthine (100 mg, 0.349 mmol) was reacted with *N*-(5-bromopyridin-3-yl)-4-methyl-*N*-tosylbenzenesulfonamide (252 mg, 0.524 mmol) according to GP2. The residue was purified by flash column chromatography (EtOAc/CH_2Cl_2, 1:20) to produce the desired sulfonamide A8 (78 mg, 42%); ^{1}H NMR δ (300 MHz, DMSO-d_6)): 2.33 (3H, s), 3.17 (3H, s), 3.52 (3H, s), 3.81 (3H, s), 6.97 (2H, d, J = 3 Mz), 7.29 (2H, d, J = 3 Mz), 7.31 (2H, d, J = 9 Mz), 7.54 (2H, d, J = 9 Mz), 7.67 (1H, t, J = 3 Mz), 8.14 (1H, s), 8.21 (1H, s), 10.64 (1H, s); ^{13}C NMR δ (75 MHz, $CDCl_3$): 21.33, 28.02, 29.89, 55.85, 109.87, 114.71, 125.39, 126.90, 127.00, 128.04, 129.31, 130.22, 136.36, 142.02, 144.16, 144.61, 147.64, 148.15, 151.25, 153.89, 160.13; HRMS (EI+) m/z calcd for $C_{26}H_{25}N_6O_5S$ $[M+H]^+$: 533.1607, found: 533.1595.

4.1.18. 7-(3,4-Dimethoxyphenyl)-8-(4-(dimethylamino)phenyl)-1,3-dimethyl-1H-purine-2,6(3H,7H)-dione (B1)

7-(3,4-Dimethoxyphenyl)-1,3-dimethyl-1H-purine-2,6(3H,7H)-dione (100 mg, 0.316 mmol) was reacted with 4-bromo-*N*,*N*-dimethylaniline (95 mg, 0.474 mmol) to GP2. After removal of palladium by filteration through Celite pad, solution was washed and dried. The residue was purified by flash column chromatography (CH_2Cl_2/MeOH, 30:1) to produce the desired aniline **B1** (68 mg, 49%); ^{1}H NMR δ (300 MHz, $CDCl_3$): 2.96 (6H, s), 3.35 (3H, s), 3.69 (3H, s), 3.80 (3H, s), 3.93 (3H, s), 6.53 (2H, d), 6.83 (1H, d), 6.93 (2H, d), 7.37 (2H, d); ^{13}C NMR δ (75 MHz, $CDCl_3$): 28.04, 29.93, 40.10, 56.13, 56.26, 108.97, 111.04, 111.39, 111.44, 115.58, 120.32, 129.49, 130.24, 148.91, 149.36, 149.70, 151.27, 151.96, 152.42, 154.41; HRMS (ESI+) m/z calcd for $C_{23}H_{25}N_5O_4$ $[M+H]^+$: 436.1979, found: 436.1969.

4.1.19. N-(4-(7-(3,4-Dimethoxyphenyl)-1,3-dimethyl-2,6-dioxo-2,3,6,7-tetrahydro-1H-purin-8-yl)phenyl)acetamide (B2)

7-(3,4-Dimethoxyphenyl)-1,3-dimethyl-1H-purine-2,6(3H,7H)-dione (100 mg, 0.316 mmol) was reacted with *N*-(4-bromophenyl)acetamide (203 mg, 0.948 mmol) to GP2. After removal of palladium by filteration through Celite pad, solution was washed and dried. The residue was subjected to HPLC separation to produce the desired acetamide **B2** (62 mg, 44%); ^{1}H NMR δ (300 MHz, $CDCl_3$): 2.11 (3H, s), 3.35 (3H, s), 3.67 (3H, s), 3.76 (3H, s), 3.89 (3H, s), 6.79 (1H, s), 6.87 (2H, s), 7.43 (4H, m), 7.80 (1H, s); ^{13}C NMR δ (75 MHz, $CDCl_3$): 24.50, 27.99, 29.82, 55.95, 56.09, 109.29, 110.88, 111.00, 119.04, 119.99, 123.74, 128.52, 129.80, 139.70, 148.49, 149.25, 149.77, 150.83, 151.67, 154.33, 168.56; HRMS (ESI+) m/z calcd for $C_{23}H_{25}N_5O_4$ $[M+H]^+$: 436.1979, found: 436.1969.

4.1.20. N-(4-(1,3-Dimethyl-2,6-dioxo-7-phenyl-2,3,6,7-tetrahydro-1H-purin-8-yl)phenyl)acetamide (C1)

1,3-Dimethyl-7-phenyl-1H-purine-2,6(3H,7H)-dione (100 mg, 0.390 mmol) was reacted with *N*-(4-bromophenyl)acetamide (250 mg, 1.171 mmol) to GP2. After removal of palladium by filteration through Celite pad, solution was washed and dried. The residue was purified by flash column chromatography (CH_2Cl_2/MeOH, 20:1) to produce the desired acetamide **C1** (98 mg, 65%); ^{1}H NMR δ (300 MHz, CD_2Cl_2): 2.11 (3H, s), 3.35 (3H, s), 3.67 (3H, s), 3.76 (3H, s), 3.89 (3H, s), 6.79 (1H, s), 6.87 (2H, s), 7.43 (4H, m), 7.80 (1H, s); ^{13}C NMR δ (75 MHz, CD_2Cl_2): 24.50, 27.99, 29.82, 55.95, 56.09, 109.29, 110.88, 111.00, 119.04, 119.99, 123.74, 128.52, 129.80, 139.70, 148.49, 149.25, 149.77, 150.83, 151.67, 154.33, 168.56; HRMS (ESI+) m/z calcd for $C_{23}H_{25}N_5O_4$ $[M+H]^+$: 436.1979, found: 436.1969.

4.1.21. N-(4-(1,3-Dimethyl-2,6-dioxo-7-p-tolyl-2,3,6,7-tetrahydro-1H-purin-8-yl)phenyl)acetamide (C2)

1,3-Dimethyl-7-p-tolyl-1H-purine-2,6(3H,7H)-dione (150 mg, 0.55 mmol) was reacted with *N*-(4-bromophenyl)acetamide (176 mg, 0.83 mmol) according to GP2. The residue was purified by flash column chromatography (CH_2Cl_2/MeOH, 50:1) to produce the desired acetamide **C2** (143 mg, 64%); ^{1}H NMR δ (300 MHz, DMSO-d_6): 2.03 (3H, s), 2.39 (3H, s), 3.17 (3H, s), 3.53 (3H, s), 7.28 (4H, m), 7.30 (2H, d, J = 8 Hz), 7.50 (2H, d, J = 8 Hz); ^{13}C NMR δ (75 MHz, DMSO-d_6): 20.75, 24.02, 27.59, 29.50, 108.58, 118.26, 122.55, 127.65, 129.52, 133.23, 138.81, 140.69, 147.95, 150.28, 153.41, 168.64; HRMS (EI+) m/z calcd for $C_{22}H_{22}N_5O_3$ $[M+H]^+$: 404.1722, found: 404.1695.

4.1.22. 8-(4-(Dimethylamino)phenyl)-7-(3-fluoro-4-methoxyphenyl)-1,3-dimethyl-1H-purine-2,6(3H,7H)-dione (D1)

7-(3-Fluoro-4-methoxyphenyl)-1,3-dimethyl-1*H*-purine-2,6(3H,7H)-dione(55 mg, 0.181 mmol) was reacted with 4-bromo-*N*,*N*-dimethylaniline(54 mg, 0.271 mmol) according to GP1. After removal of palladium by filteration through Celite, solution was washed and dried. The residue was purified by flash column chromatography (CH_2Cl_2/MeOH, 20:1) to produce the desired product **D1** (87 mg, 53%); ^{1}H NMR δ (300 MHz, $CDCl_3$): 2.96 (6H, s), 3.34 (3H, s), 3.67 (3H, s), 3.93 (3H, s), 6.53 (2H, d), 7.00 (1H, t), 7.08 (2H, m), 7.31 (2H, d); ^{13}C NMR δ (75 MHz, $CDCl_3$): 27.92, 29.84, 39.98, 56.32, 108.69, 111.38, 113.02, 115.02, 116.13, 124.01, 128.94, 130.22, 148.39, 148.88, 150.54, 151.25, 151.76, 152.49, 153.01, 154.34; HRMS (ESI+) m/z calcd for $C_{22}H_{23}FN_5O_3$ $[M+H]^+$: 424.1785, found: 424.1797.

4.1.23. N-(4-(7-(3-Fluoro-4-methoxyphenyl)-1,3-dimethyl-2,6-dioxo-2,3,6,7-tetrahydro-1H-purin-8-yl)phenyl)acetamide (D2)

7-(3-Fluoro-4-methoxyphenyl)-1,3-dimethyl-1H-purine-2,6(3H,7H)-dione (200 mg, 0.675 mmol) was reacted with *N*-(4-bromophenyl)acetamide (0.211 mg, 0.986 mmol) according to GP1. After removal of palladium by filteration through Celite, solution was washed and dried. The residue was purified by flash column chromatography (CH_2Cl_2/MeOH, 15:1) to produce the desired acetamide **D2** (168 mg, 57%); ^{1}H NMR δ (300 MHz,, $CDCl_3$): 2.14 (3H, s), 3.34 (3H, s), 3.68 (3H, s), 3.91 (3H, s), 7.00 (1H, t), 7.05 (2H, m), 7.33 (1H, s), 7.42 (2H, d), 7.46 (2H, d); ^{13}C NMR δ (75 MHz,, $CDCl_3$): 24.25, 27.56, 29.43, 55.83, 108.74, 122.56, 115.47, 118.65, 123.12, 127.60, 129.54, 139.22, 148.14, 150.01, 150.46, 151.17, 152.50, 153.97, 167.88; HRMS (ESI+) m/z calcd for $C_{22}H_{20}FN_5NaO_4$ $[M+Na]^+$: 460.1367, found: 460.1428.

4.1.24. 1-(4-(7-(3-Fluoro-4-methoxyphenyl)-1,3-dimethyl-2,6-dioxo-2,3,6,7-tetrahydro-1H-purin-8-yl)phenyl)-3-methylurea (D3)

7-(3-Fluoro-4-methoxyphenyl)-1,3-dimethyl-1*H*-purine-2,6-(3H,7H)-dione(180 mg, 0.592 mmol) was reacted with 1-(4-bromophenyl)-3-methylurea(203 mg, 0.887 mmol) according to GP1. After removal of palladium by filteration through Celite, solution was washed and dried. The residue was purified by flash column chromatography (CH_2Cl_2/MeOH, 20:1) to produce the desired urea **D3** (166 mg, 62%); ^{1}H NMR δ (300 MHz, DMSO-d_6): 2.60 (2H, d), 3.16 (2H, s), 3.52 (2H, s), 3.89 (3H, s), 6.10 (1H, d), 7.14 (1H, dd), 7.21 (1H, t), 7.27 (2H, m), 7.34 (2H, m), 7.44 (1H, dd), 8.74 (1H, s); ^{13}C NMR δ (75 MHz, DMSO-d_6): 26.18, 27.59, 29.50, 56.18, 108.58, 113.36, 116.17, 116.88, 120.22, 124.63, 128.18, 129.58, 142.38, 143.38, 147.72, 149.33, 150.87, 151.78, 153.42, 155.42; HRMS (ESI+) m/z calcd for $C_{22}H_{22}FN_6O_4$ $[M+H]^+$: 453.1681, found: 453.1718.

4.1.25. N-(4-(7-(3-Fluoro-4-methoxyphenyl)-1,3-dimethyl-2,6-dioxo-2,3,6,7-tetrahydro-1H-purin-8-yl)-2-methoxyphenyl) acetamide (D4)

7-(3-Fluoro-4-methoxyphenyl)-1,3-dimethyl-1*H*-purine-2,6-(3H,7H)-dione (100 mg, 0.329 mmol) was reacted with *N*-(4-bromo-2-methoxyphenyl)acetamide (121 mg, 0.493 according to

GP2. After removal of palladium by filteration through Celite, solution was washed and dried. The residue was and subjected to HPLC separation to produce the desired amide **D4** (110 mg, 72%); ^{1}H NMR δ (400 MHz, $CDCl_3$): 2.18 (3H, s), 3.35 (3H, s), 3.68 (3H, s), 3.78 (3H, s), 3.92 (3H, s), 6.91 (1H, dd), 7.02 (1H, t), 7.07 (2H, m), 7.12 (1H, d), 7.78 (1H, s), 8.26 (1H, d); ^{13}C NMR δ (100 MHz, $CDCl_3$): 25.14, 28.17, 30.09, 55.88, 56.52, 109.43, 110.72, 113.23, 116.16, 119.12, 122.58, 123.03, 124.05, 128.46, 129.81, 147.34, 148.72, 150.71, 151.22, 151.82, 154.59, 168.44; HRMS (ESI+) *m*/*z* calcd for $C_{23}H_{23}FN_5O_5$ $[M+H]^+$: 467.1678, found: 467.1673.

4.1.26. 8-(4-(Dimethylamino)phenyl)-7-(3-fluorophenyl)-1,3-dimethyl-1H-purine-2,6(3H,7H)-dione (E1)

7-(3-Fluorophenyl)-1,3-dimethyl-1*H*-purine-2,6(3H,7H)-dione (80 mg, 0.292 mmol) was reacted with 4-bromo-*N*,*N*-dimethylaniline(0.088 mg, 0.438 mmol) according to GP2. After removal of palladium by filteration through Celite, solution was washed and dried. The residue was purified by flash column chromatography (CH_2Cl_2/MeOH, 20:1) to produce the desired aniline **E1** (70 mg, 57%); ^{1}H NMR δ (300 MHz, $CDCl_3$): 2.95 (6H, s), 3.34 (3H, s), 3.67 (3H, s), 6.51 (2H, d), 7.06 (1H, s), 7.17 (2H, t), 7.28 (2H, d), 7.41 (1H, q); ^{13}C NMR δ (75 MHz, $CDCl_3$): 27.94, 29.88, 39.96, 108.49, 111.32, 114.79, 115.60, 116.34, 123.89, 130.23, 137.65, 148.99, 151.25, 151.71, 152.39, 154.24, 161.24, 163.72; HR-MS (ESI+) *m*/*z* calcd for $C_{21}H_{20}FN_5NaO_2$ $[M+Na]^+$: 416.1499, found: 416.1525.

4.1.27. N-(4-(7-(3-Fluorophenyl)-1,3-dimethyl-2,6-dioxo-2,3,6,7-tetrahydro-1H-purin-8-yl)phenyl)acetamide (E2)

Aryl xanthine (36 mg, 0.132 mmol) was reacted with *N*-(4-bromophenyl)acetamide (42 mg, 0.197 mmol) according to GP2. The residue was purified by flash column chromatography (CH_2Cl_2/MeOH, 20:1) to produce the desired acetylamide **E2** (25 mg, 48%); ^{1}H NMR δ (300 MHz, $CDCl_3$): 2.14 (3H, s), 3.43 (3H, s), 3.67 (3H, s), 7.02 (1H, m), 7.10 (1H, d), 7.17 (1H, m), 7.37(5H, dd); ^{13}C NMR δ (75 MHz, $CDCl_3$): 24.64, 28.00, 29.88, 108.97, 115.67, 116.63, 119.06, 123.40, 129.98, 130.51,,136.85, 139.85, 148.71, 150.80, 151.55, 154.30, 160.76, 164.07, 168.28; HRMS (EI+) *m*/*z* calcd for $C_{21}H_{19}FN_5O_3$ $[M+H]^+$: 408.1472, found: 408.1465.

4.1.28. 8-(4-(Dimethylamino)-2-methoxyphenyl)-7-(3-fluorophenyl)-1,3-dimethyl-1H-purine-2,6(3H,7H)-dione (E3)

7-(3-Fluorophenyl)-1,3-dimethyl-1*H*-purine-2,6(3H,7H)-dione (120 mg, 0.438 mmol) was reacted with 4-bromo-3-methoxy-*N*,*N*-dimethylaniline (201 mg, 0.875 mmol) according to GP2. After removal of palladium by filteration through Celite, solution was washed and dried. The residue was purified by flash column chromatography (CH_2Cl_2/MeOH, 20:1) to produce the desired product **E3** (70 mg, 57%); ^{1}H NMR δ (300 MHz, $CDCl_3$): 2.95 (6H, s), 3.31 (3H, s), 3.37 (3H, s), 3.66 (2H, s), 5.90 (1H, s), 6.31 (1H, dd), 6.96 (1H, dd), 7.01 (1H, dd), 7.28 (1H, q), 7.33 (1H, d); ^{13}C NMR δ (75 MHz, $CDCl_3$): 27.94, 29.84, 40.09, 54.19, 94.12, 104.60, 107.72, 114.26, 114.94, 122.63, 128.88, 132.39, 137.53, 148.85, 151.56, 153.44, 154.24, 157.58, 160.52, 162.97, 163.85; HRMS (ESI+) *m*/*z* calcd for $C_{22}H_{23}FN_5O_3$ $[M+H]^+$: 424.1785, found: 424.1830.

4.1.29. 7-(3,5-Difluorophenyl)-8-(4-(dimethylamino)phenyl)-1,3-dimethyl-1H-purine-2,6(3H,7H)-dione (F1)

7-(3,5-Difluorophenyl)-1,3-dimethyl-1*H*-purine-2,6(3H,7H)-dione (100 mg, 0.342 mmol) was reacted with 4-bromo-*N*,*N*-dimethylaniline (103 mg, 0.513 mmol) to GP2. After removal of palladium by filteration through Celite pad, solution was washed and dried. The residue was subjected to HPLC separation to produce the desired product **F1** (69 mg, 50%); ^{1}H NMR δ (300 MHz, $CDCl_3$): 2.99 (6H, s), 3.37 (3H, s), 3.69 (3H, s), 6.57 (2H, d), 6.93 (2H, d), 6.97 (1H, br), 7.32 (2H, d); ^{13}C NMR δ (75 MHz, $CDCl_3$): 27.99, 29.67, 29.91, 39.94, 105.19, 108.36, 111.43, 112.12, 114.38, 130.22, 138.39, 149.10, 151.45, 151.66, 152.54, 154.17, 162.68 (dd); HRMS (ESI+) *m*/*z* calcd for $C_{21}H_{19}F_2N_5O_2$ $[M+H]^+$: 412.1580, found: 412.1592.

4.1.30. 7-(3,4-Dichlorophenyl)-8-(4-(dimethylamino)phenyl)-1,3-dimethyl-1H-purine-2,6(3H,7H)-dione (G1)

7-(3,4-Dichlorophenyl)-1,3-dimethyl-1*H*-purine-2,6(3H,7H)-dione (100 mg, 0.308 mmol) was reacted with 4-bromo-*N*,*N*-dimethylaniline (92 mg, 0.461 mmol) to GP2. After removal of palladium by filteration through Celite pad, solution was washed and dried. The residue was purified by flash column chromatography (CH_2Cl_2/MeOH, 50:1) to produce the desired product **G1** (56 mg, 41%); ^{1}H NMR δ (300 MHz, $CDCl_3$) 2.99 (6H, s), 3.37 (3H, s), 3.69 (3H, s), 6.58 (2H, d), 7.21 (1H, dd), 7.32 (2H, d), 7.48 (1H, s), 7.53 (1H, d); ^{13}C NMR δ (75 MHz, DMSO-d_6): 28.08, 29.98, 55.33, 55.90, 109.48, 114.65, 120.29, 121.53, 124.46, 128.61, 129.44, 132.50, 139.25, 148.25, 150.49, 151.40, 154.01, 159.98, 167.00; HRMS (ESI+) *m*/*z* calcd for $C_{21}H_{22}N_5O5_S$ $[M+H]^+$: 456.1336, found: 456.1355.

4.1.31. N-(4-(7-(3,4-Dichlorophenyl)-1,3-dimethyl-2,6-dioxo-2,3,6,7-tetrahydro-1H-purin-8-yl)phenyl)acetamide (G2)

7-(3,4-Dichlorophenyl)-1,3-dimethyl-1*H*-purine-2,6(3H,7H)-dione (100 mg, 0.308 mmol) was reacted with *N*-(4-bromophenyl)acetamide (198 mg, 0.924 mmol) to GP2. After removal of palladium by filteration through Celite pad, solution was washed and dried. The residue was purified by flash column chromatography (CH_2Cl_2/MeOH, 50:1) to produce the desired product **G2** (38 mg, 41%); ^{1}H NMR δ (300 MHz, $CDCl_3$): 2.16 (3H, s), 3.36 (3H, s), 3.68 (3H, s), 7.17 (1H, dd), 7.39 (2H, d), 7.44 (2H, d), 7.51 (2H, dd), 7.65 (1H, s); ^{13}C NMR δ (75 MHz, $CDCl_3$): 24.78, 28.24, 30.11, 109.02, 119.42, 123.20, 127.27, 129.83, 130.22, 131.05, 133.50, 134.29, 135.06, 140.23, 149.00, 151.13, 151.69, 154.51, 168.66; HRMS (ESI+) m/z calcd for $C_{21}H_{17}Cl_2N_5O_3$ $[M+H]^+$: 456.1336, found: 456.1355.

4.1.32. N-(4-(7-(3,4-Dichlorophenyl)-1,3-dimethyl-2,6-dioxo-2,3,6,7-tetrahydro-1H-purin-8-yl)-3-methoxyphenyl)acetamide (G3)

7-(3,4-Dichlorophenyl)-1,3-dimethyl-1*H*-purine-2,6(3H,7H)-dione (100 mg, 0.308 mmol) was reacted with *N*-(4-bromo-3-methoxyphenyl)acetamide (226 mg, 0.924 mmol) to GP2. After removal of palladium by filteration through Celite pad, solution was washed and dried. Crude The residue was subjected to HPLC separation to produce the desired product **G3** (62 mg, 41%); ^{1}H NMR δ (300 MHz, $CDCl_3$): 2.14 (3H, s), 3.38 (3H, s), 3.42 (3H, s), 3.66 (3H, s), 6.88 (1H, dd), 7.04 (1H, dd), 7.40 (4H, m), 7.79 (1H, s); ^{13}C NMR δ (75 MHz, $CDCl_3$): 24.81, 28.26, 29.78, 30.13, 55.02, 102.49, 108.28, 111.35, 112.57, 126.18, 128.93, 129.95, 132.29, 133.07, 135.11, 142.43, 148.97, 150.45, 151.66, 154.51, 157.37, 168.88; HRMS (ESI+) *m*/*z* calcd for $C_{22}H_{19}Cl_2N_5O_4$ $[M+H]^+$: 488.0887, found: 488.0922.

4.2. Biological assays and methods

4.2.1. PI3-Kinase assay

The PI3K assay was performed using the Kinase-Glo® Max luminescent kinase assay kit (Promega Cat. # V6073) which quantifies the amount of ADP produced by the PI3K reaction. In brief, an active PI3K (100 ng) was preincubated with compound for 5 min in kinase reaction buffer (25 mM MOPS [pH 7.0], 5 mM $MgCl_2$, and 1 mM EGTA) and 10 μg L-α-phosphatidylinositol (PI) (Sigma Cat. # P8443). Before addition of PI, it was sonicated with sonication buffer (25 mM MOPS [pH 7.0], 1 mM EGTA) in water for 20 min

for allowing miscelle formation. Then reaction was started by the addition of 10 μM ATP and ran for 180 min. To terminate kinase reaction, same volume of Kinase-Glo® Max buffer was added. After 10 min, the plates were then read on a GloMax plate reader for luminescence detection.

4.2.2. MTT assay

Cell viability was performed by a MTT assay. Briefly, T47D cells were plated at a density of 5×10^3 cells/well in 96-well plates for 24 h. Then, the medium was removed, and cells were treated with either DMSO as a control or various concentrations of inhibitors. The final concentration of DMSO in the medium was $\leqslant$0.1% (v/v). After the cells were incubated for 482 h, 20 μl MTT solution (5 mg/ml) was added to each well for another 4 h at 37C. The formazan crystals that formed were dissolved in DMSO (100 μl/well) by constant shaking for 5 min. The plate was then read on a microplate reader at 540 nm. Three replicate wells were used for each analysis. The median inhibitory concentration (IC_{50}, defined as the drug concentration at which cell growth was inhibited by 50%) was assessed from the dose-response curves. To assess the effect of compounds on cell proliferation, T47D cells were cultured with compound (0.1–100 μM) for 48 h before MTT analysis.

4.2.3. Absolute quantum yield measurement

Absolute quantum yields (Φ_F) were measured by combination system of Spectrophotometer (V-530 UV–vis Spectrophotometer, JASCO, Inc.) with Fluorimeter (RF-5301PC Spectro-fluorophotometer, SHIMADZU Corp.) Sample was prepared as solution by dilution of fluorescent compound in DCM. Absorption λ_{max} was measured with spectrophotometer from scanning 700–250 range wavelength while fluorescence emission λ_{max} and integrated intensity was analyzed with OriginPro 8 software. Absolute quantum yield of known fluorescent dye––Fluorescein––was obtained to bring out those of samples precisely. ($\Phi_F = 0.925 \pm 0.015$ in 0.1 N NaOH aqueous solution).

Acknowledgments

This research was supported by National Research Foundation of Korea (NRF) through general research grants (NRF-2010-0015340 and 2010-0022179), by the Korean Health Technology R&D Project (A101185), and by the National R&D Program for Cancer Control (1020250), Ministry for Health, Welfare and Family Affairs, Korea.

References and notes

1. (a) Quah, B. J. C.; Warren, H. S.; Parish, C. R. *Nat. Protoc.* **2007**, *2*, 2049; (b) Boonyarattanakalin, S.; Hu, J.; Dykstra-Rummel, S.; August, A.; Peterson, B. R. *J. Am. Chem. Soc.* **2007**, *129*, 268; (c) Bae, Y.; Nishiyama, N.; Fukushima, S.; Koyama, H.; Yasuhiro, M.; Kataoka, K. *Bioconjugate Chem.* **2005**, *16*, 122.
2. (a) Tanabe, K.; Zhang, Z.; Ito, T.; Hatta, H.; Nishimoto, S. *Org. Biomol. Chem.* **2007**, *5*, 3745; (b) Son, J.; Lee, J.-J.; Lee, J.-S.; Schuller, A.; Chang, Y.-T. *ACS Chem. Bio.* **2010**, *5*, 449.
3. Safaei, R.; Kantano, K.; Larson, B. J.; Samimi, G.; Holzer, A. K.; Naerdemann, W.; Tomioka, M.; Goodman, M.; Howell, S. B. *Clin. Cancer Res.* **2005**, *11*, 756.
4. (a) Uddin, M. J.; Crews, B. C.; Blobaum, A. L.; Kingsley, P. J.; Gorden, D. L.; McIntyre, J. O.; Matrisian, L. M.; Subbaramaiah, K.; Dannenberg, A. J.; Piston, D. W.; Marnett, L. J. *Cancer. Res.* **2010**, *70*, 3618; (b) Yee, M.-C.; Fas, S. C.; Stohlmeyer, M. M.; Wandless, T. J.; Cimprich, K. A. *J. Biol. Chem.* **2005**, *280*, 29053; (c) Miller, L. M.; Cai, Y.; Sheetz, M. P.; Cornish, V. W. *Nature Method* **2005**, *2*, 255; (d) Miller, L. W.; Sable, J.; Goelet, P.; Sheetz, M. P.; Cornish, V. W. *Angew. Chem., Int. Ed. Engl.* **2004**, *43*, 1672.
5. Klein, A. V.; Hambley, T. W. *Chem. Rev.* **2009**, *109*, 4911.
6. Vanhaesebroeck, B.; Leevers, S. J.; Khatereh, A.; Timms, J.; Katso, R.; Driscoll, P. C.; Woscholski, R.; Parker, P. J.; Waterfield, M. D. *Annu. Rev. Biochem.* **2001**, *70*, 535.
7. (a) Samuels, Y.; Wang, Z.; Bardelli, A.; Silliman, N.; Ptak, J.; Szabo, S.; Yan, H.; Gazdar, A.; Powell, S. M.; Riggins, G. J.; Willson, J. K.; Markowitz, S.; Kinzler, K. W.; Vogelstein, B.; Velculescu, V. E. *Science* **2004**, *304*, 554; (b) Parsons, D. W.; Wang, T.-L.; Samuels, Y.; Bardelli, A.; Cummins, J. M.; DeLong, L.; Silliman, N.; Ptak, J.; Szabo, S.; Willson, J. K.; Markowitz, S.; Kinzler, K. W.; Vogelstein, B.; Lengauer, C.; Velculescu, V. E. *Nature* **2005**, *436*, 792; (c) Kang, S.; Bader, A. G.; Vogt, P. K. *Proc. Natl. Acad. Sci. U.S.A.* **2005**, *102*, 802; (d) Fan, Q.-W.; Knight, A. A.; Goldenberg, D. D.; Yu, W.; Mostov, K. E.; Stokoe, D.; Shokat, K. M.; Weiss, W. A. *Cancer Cell* **2006**, *9*, 341; (e) Ward, S.; Sotsios, Y.; Dowden, J.; Bruce, I.; Finan, P. *Chem. Biol.* **2003**, *10*, 207; (f) Ward, S. G.; Finan, P. *Curr. Opin. Pharmacol.* **2003**, *3*, 426; (g) Hong, S.; Lee, S.; Kim, B.; Lee, H.; Hong, S.-S.; Hong, S. *Bioorg. Med. Chem. Lett.* **2010**, *20*, 7212.
8. O'Brien, C.; Wallin, J. J.; Sampath, D.; Guhathakurta, D.; Savage, H.; Punnoose, E. A.; Guan, J.; Berry, L.; Prior, W. W.; Amler, L. C.; Belvin, M.; Friedman, L.; Lackner, M. *Clin. Cancer. Res.* **2010**, *16*, 3670.
9. Kim, D.; Jun, H.; Lee, H.; Hong, S.-S.; Hong, S. *Org. Lett.* **2010**, *12*, 1212.
10. (a) Maira, S.-M.; Stauffer, F.; Brueggen, J.; Furet, P.; Schnell, C.; Fritsch, C.; Brachmann, S.; Chene, P.; Pover, A. D.; Schoemaker, K.; Fabbro, D.; Gabriel, D.; Simonen, M.; Murphy, L.; Finan, P.; Sellers, W.; Garcıa-Echeverrıa, C. *Mol. Cancer Ther.* **2008**, *7*, 1851; (b) Cherian, P. T.; Koikov, L. N.; Wortman, M. D.; Knittel, J. J. *Bioorg. Med. Chem. Lett.* **2009**, *19*, 2215.
11. Full IC_{50} values against PI3Kα using PI3-Kinase Glo kit (Promega-inc). Cell viability was tested using MTT assay.
12. Zhao, D.; Wang, W.; Yang, F.; Lan, J.; Yang, L.; Gao, G.; You, J. *Angew. Chem., Int. Ed. Engl.* **2009**, *48*, 3296.
13. (a) Signore, G.; Nifosi, R.; Albertazzi, L.; Storti, B.; Bizzarri, R. *J. Am. Chem. Soc.* **2010**, *132*, 1276; (b) Kim, E.; Koh, M.; Ryu, J.; Park, S. *J. Am. Chem. Soc.* **2008**, *130*, 12206.